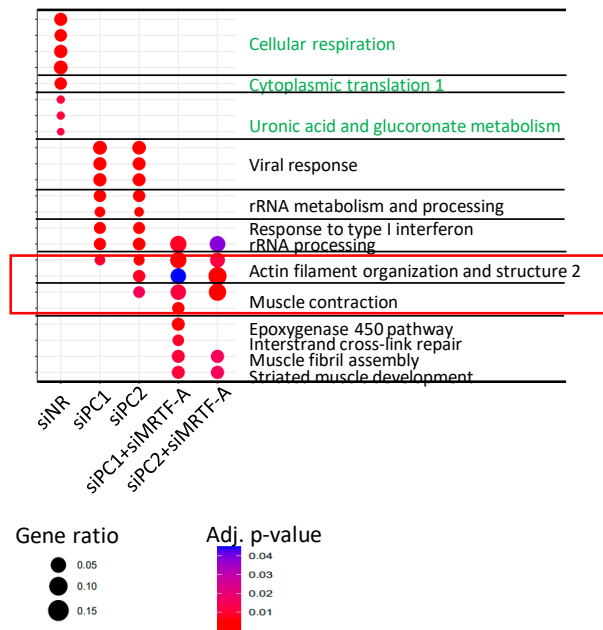
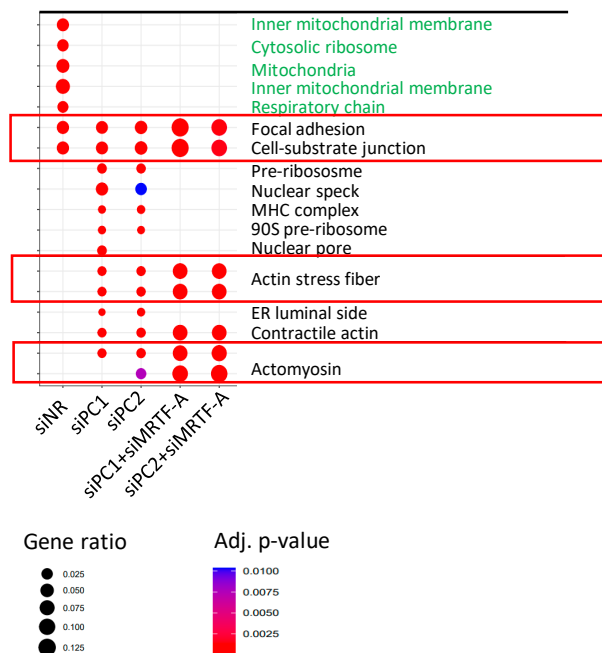


Supplementary Figure S1. Experimental setup. (A) siPC1-1433 and siPC2-1644 are a second set of *PC1*- and *PC2*-targeting siRNAs (respectively). Transfection of either siPC1-1433 (150 nM) or PC2-1644 (100 nM) enhanced *TAGLN* expression. qPCR data are shown. (B) *MRTF-A* mRNA was quantified by RT-qPCR. siPC1 or siPC2 knockdown did not alter the efficiency of *MRTF-A* silencing (n = 3, n.s. non-significant, ** $p < 0.01$, *** $p < 0.001$).

A Biological processes

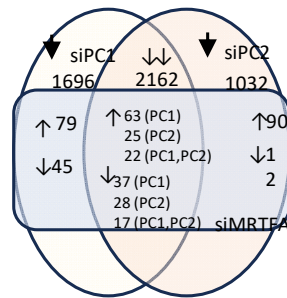


B Cellular compartment



Supplementary Figure S2. PKD-linked cytoskeletal changes are regulated by MRTF. Differentially expressed genes were determined as detailed in Supplementary Methods, and were subjected to enrichment analysis of Biological Processes (A) and Cellular Compartment (B), using ClusterProfiler in R. Categories that were depleted in siPC1 and siPC2 conditions (compared to siNR) are shown in green. Further, selected top categories that were enriched in siPC1 and siPC2 conditions (compared to siNR) are listed in the siPC1 and siPC2 columns. Significant decreases compared to these in siMRTF-treated samples are shown in the next two columns. Note that biological processes that overlap between PC knockdown conditions and the siPC+siMRTF-A conditions were related to cytoskeleton organization and cell contractility (red rectangles).

Genes and GO categories underrepresented upon PC loss



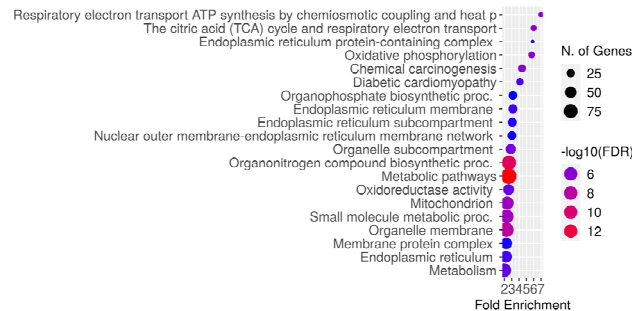
siNR vs siPC1 ↓: 3982
 siNR vs siPC2 ↓: 3296
 siNR vs siPC1 ↓ siNR vs siPC2 down: 2262

siNR vs siPC1 ↓, AND siPC1 vs siPC1+siMRTF-A ↑: 164
 siNR vs siPC1 ↓, AND siPC1 vs siPC1+siMRTF-A ↓: 82

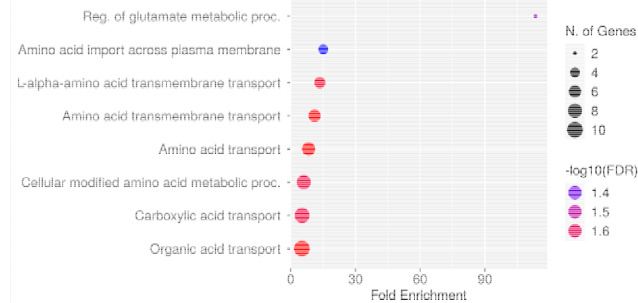
siNR vs siPC2 ↓, AND siPC2 vs siPC2+siMRTF-A ↑: 153
 siNR vs siPC2 ↓, AND siPC2 vs siPC2+siMRTF-A ↓: 49

siNR vs siPC1, siPC2 ↓, AND siPC1 vs siPC1+siMRTF-A ↑: 85
 siNR vs siPC1, siPC2 ↓, AND siPC1 vs siPC1+siMRTF-A ↓: 54
 siNR vs siPC1, siPC2 ↓, AND siPC2 vs siPC2+siMRTF-A ↑: 47
 siNR vs siPC1, siPC2 ↓, AND siPC2 vs siPC2+siMRTF-A ↓: 45
 siNR vs siPC1, siPC2 ↓, AND siPC1,2 vs siPC1,2+siMRTF-A ↑: 22
 siNR vs siPC1, siPC2 ↓, AND siPC1,2 vs siPC1,2+siMRTF-A ↓: 17

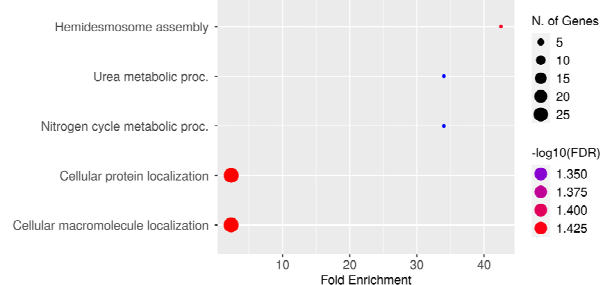
Biological processes downregulated by both PC1- and PC2 loss



Biological processes downregulated by PC1-loss and partially restored by MRTF-A downregulation

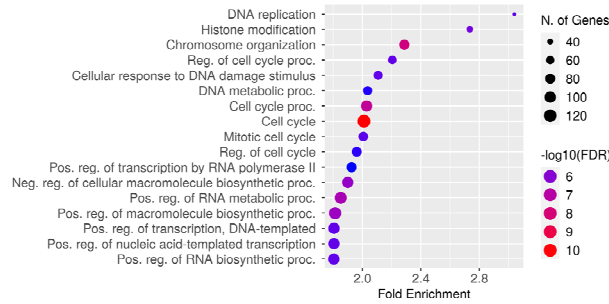


Biological processes downregulated by PC2-loss and partially restored by MRTF-A downregulation

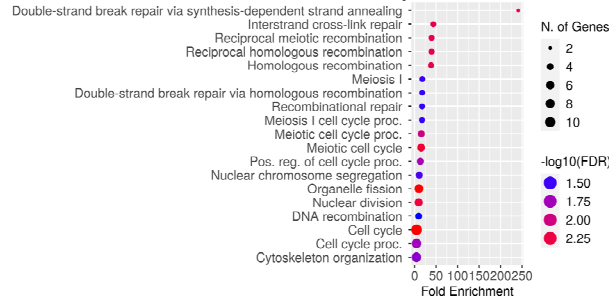


Supplementary Figure S3. PC1 and PC2 loss-specific underrepresented biological processes and their MRTF-dependence. Top panel: Epithelial cells knocked down for PC1 and PC2 transcriptionally underrepresented several metabolic pathways. Lower panels: Out of these, MRTF-A silencing partially mitigates amino acid transport across plasma membrane (siPC1).

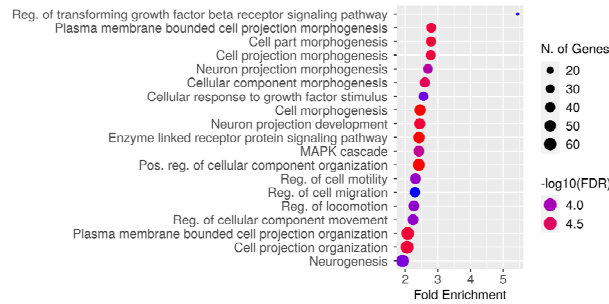
Selectively upregulated biological processes by PC1 loss



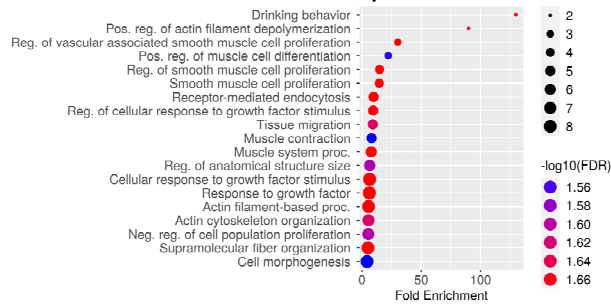
MRTF-A-dependent subset of the above



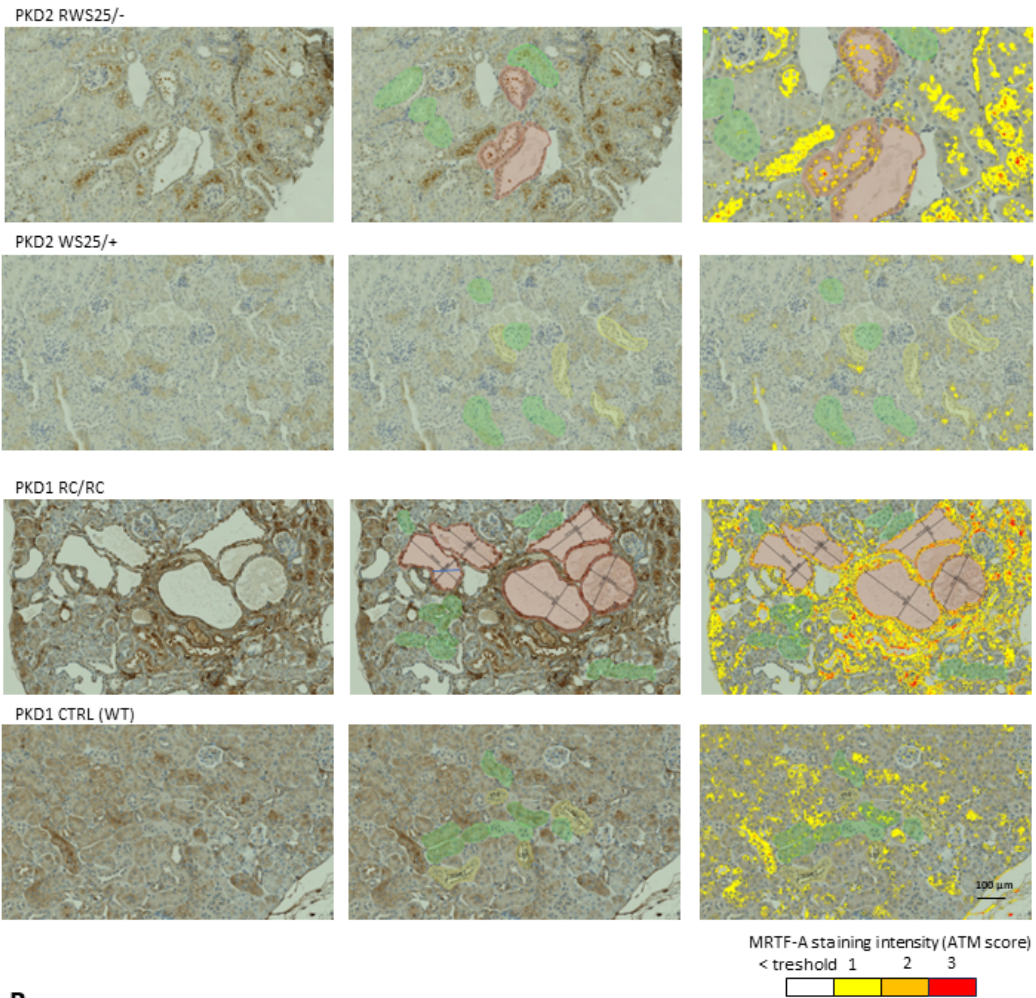
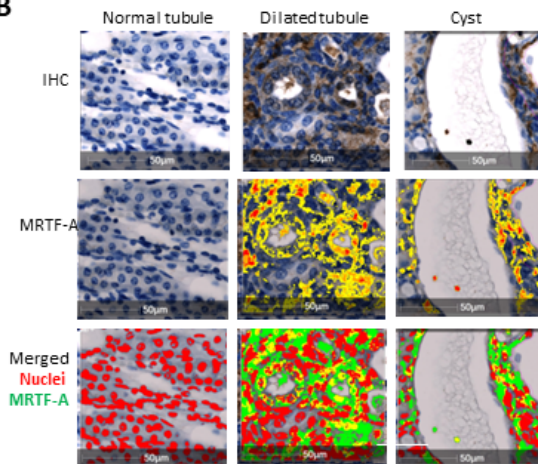
Selectively upregulated biological processes by PC1 loss



MRTF-A-dependent subset of the above



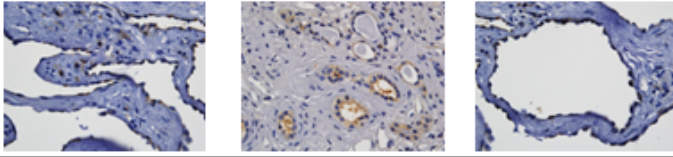
Supplementary Figure S4. PC1 and PC2 loss-specific biological processes. DEG searched for transcripts that were upregulated upon PC1 loss but were unaffected by PC2 loss, or vice versa. For PC1, loss-related biological processes centered around DNA replication and transcription (top panel). Within this transcript set, MRTF-dependent genes were grouped in DNA recombination-related repair. Interestingly, PC2-specific upregulated categories remained to be linked to cell projection/cytoskeletal reorganization/cell motility. The MRTF-dependent subset is predicted to regulate the actin cytoskeleton, cell contractility, and muscle development.

A**B**

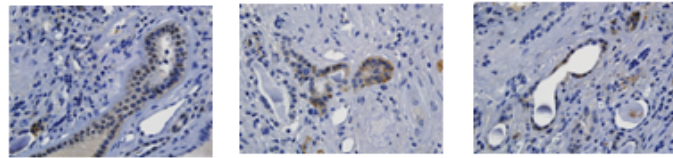
Supplementary Figure S5. Expression analysis methods. (A) ATM within the Area Quantification Module measured MRTF-A/DAB signal and colored each pixel according to its DAB optical density. Yellow to red color gradient corresponds to increasing MRTF-A expression, as indicated. Green and yellow masks show selected normal tubules without or with lumen, respectively. Red masks depict visibly enlarged tubules; lumen measurements are given in μm . Scale bar corresponds to all panels. (B) Automated Area Quantification Module was trained to recognize the hematoxylin-stained nuclei and to depict MRTF-A expression, as in (A, middle row panels). The bottom panels show a superimposed image of the nuclear mask and the MRTF-A-specific stain. Here red indicates nuclei, green indicates MRTF-A and yellow depicts nuclear MRTF-A.

MRTF-A IHC

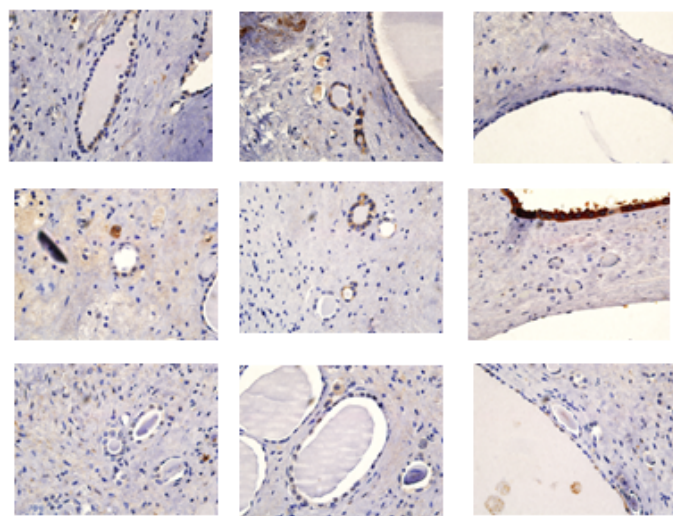
PKD Patient R



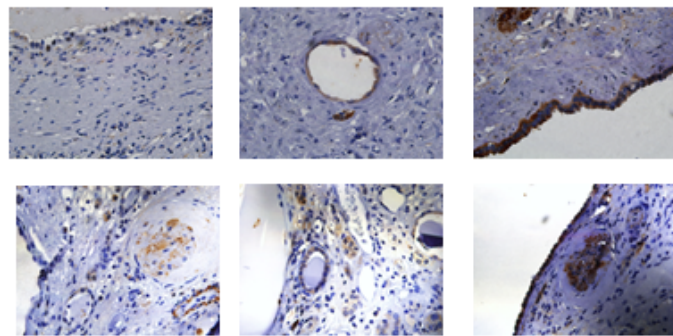
PKD Patient P



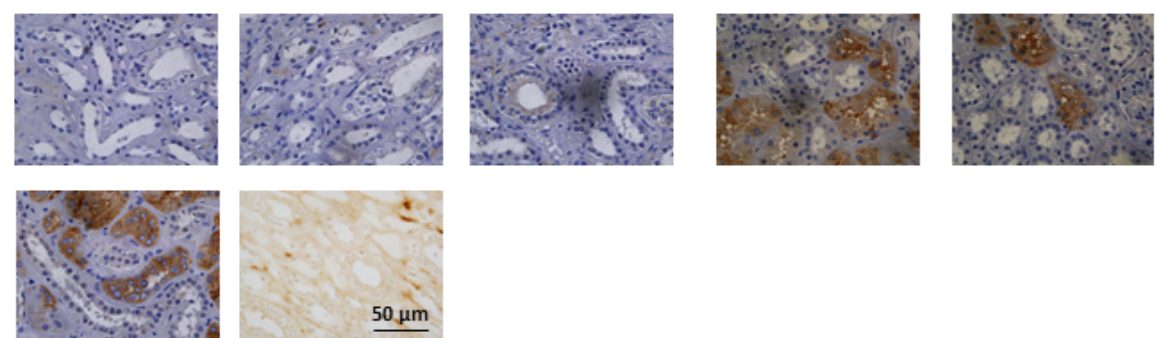
PKD Patient L



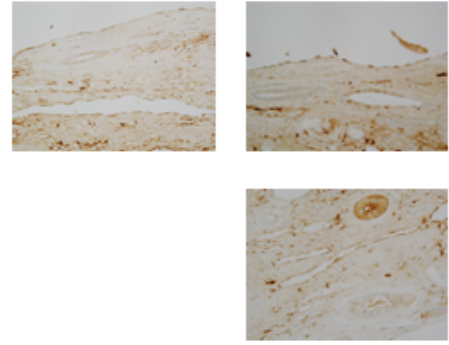
PKD Patient K



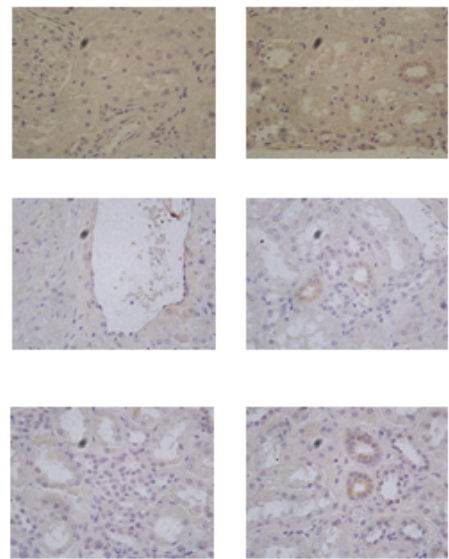
RCC Patient T



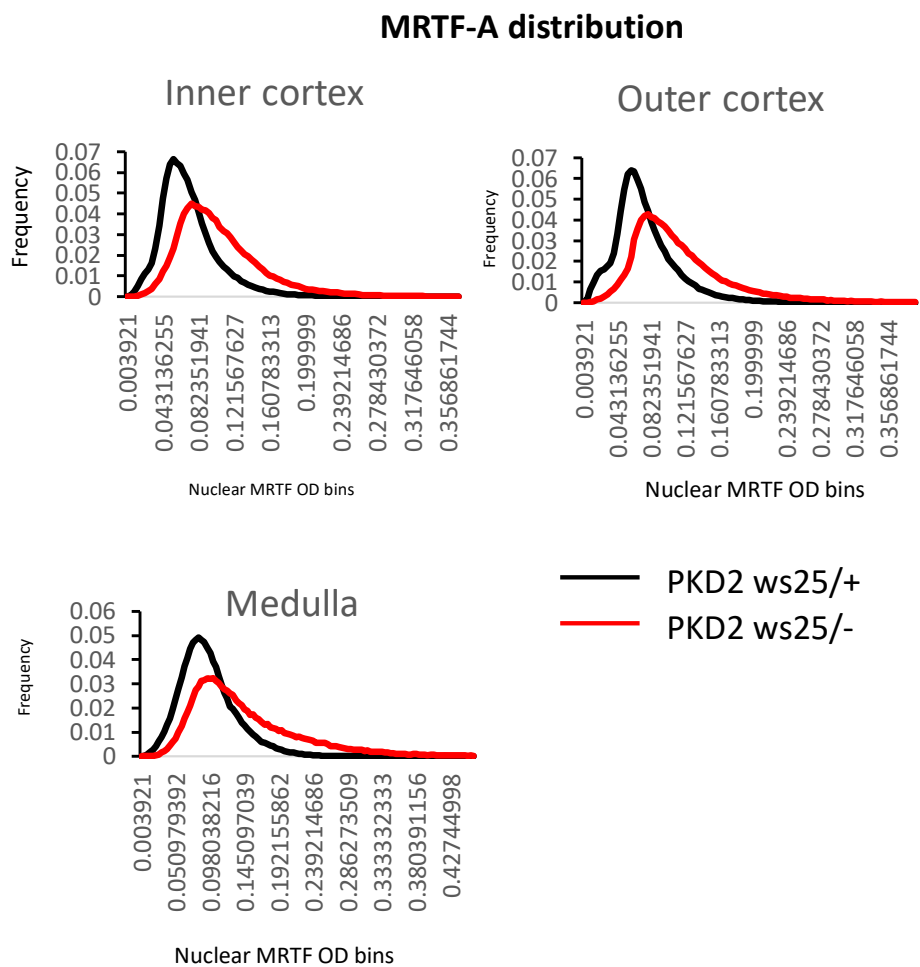
PKD Patient W



No primary antibody ctrl



Supplementary Figure S6. ADPKD patients' cystic epithelium shows enhanced MRTF-A expression. Five ADPKD patients (patient R, P, L, K, and W) and control (normal kidney tissue from a clear cell renal cell carcinoma patient) specimens were assessed for MRTF-A expression by IHC. Nuclear expression of MRTF-A was observed in all ADPKD patients, albeit the extent varied. The cystic epithelial wall showed enhanced MRTF expression compared to the normal tubules within the same patient's specimens and to the normal tubules of the RCC patient. Scale bar corresponds to all panels.



Supplementary Figure S7. Distribution curves show the frequency of nuclei with increasing MRTF-A expression. The inner cortex, outer cortex, and medulla were assessed separately in *Pkd2* *WS25/-* (3 months old, n = 5) and control *Pkd2* *WS25/+* (3 months old, n = 5) animals.